

Deep Learning Based Adaptive Joint mmWave Beam Alignment

Daniel Tandler*, Marc Gauger*, Ahmet Serdar Tan[†], Sebastian Dörner* and Stephan ten Brink*

*Institute of Telecommunications, University of Stuttgart, Pfaffenwaldring 47, 70659 Stuttgart, Germany

{tandler,gauger,doerner,tenbrink}@inue.uni-stuttgart.de

[†] InterDigital Europe, London, United Kingdom

Abstract—The challenging propagation environment, combined with the hardware limitations of mmWave systems, gives rise to the need for accurate initial access beam alignment strategies with low latency and high achievable beamforming gain. Much of the recent work in this area either focuses on one-sided beam alignment, or, joint beam alignment methods where both sides of the link perform a sequence of fixed channel probing steps. Codebook-based non-adaptive beam alignment schemes have the potential to allow multiple user equipments (UEs) to perform initial access beam alignment in parallel whereas adaptive schemes are favourable in achievable beamforming gain. This work introduces a novel deep learning based joint beam alignment scheme that aims to combine the benefits of adaptive, codebook-free beam alignment at the UE side with the advantages of a codebook-sweep based scheme at the basestation (BS). The proposed end-to-end trainable scheme is compatible with current cellular standard signaling and can be readily integrated into the standard without requiring significant changes to it. Extensive simulations demonstrate superior performance of the proposed approach over purely codebook-based ones.

I. INTRODUCTION

The need for highly directional transmissions using beamforming techniques to overcome the large pathloss at mmWave frequencies requires systems operating at these frequencies to use large antenna arrays and highly directive beamforming (BF). Due to the prohibitive cost and power consumption of fully digital systems operating at these high frequencies, mmWave systems often adopt analog or hybrid beamforming techniques. These restrictions gives rise to the need for specific initial access (IA) strategies, often called beam alignment (BA) or beam training (BT). There has been a great amount of work done in this area, many using beam-codebooks together with methods like compressed-sensing, machine learning, and Bayesian approaches [1][2][3]. Recently it has been shown that codebook-free, adaptive BA might have performance benefits over non-adaptive and codebook based approaches [4] [5] [6]. Note that much of these works focus on the problem of one-sided BA, where one side of the link sends omnidirectionally while the other side performs BA. While this can be extended in a straightforward way to two-sided BA if one assumes a time division duplex (TDD) system, this approach might not be optimal in BA latency or performance. Other works, like in [7] and [8] perform joint, two-sided BA by interpreting the BA as a adversarial bandit problem using predefined beam codebooks. Recent work [9] introduces a joint dense neural

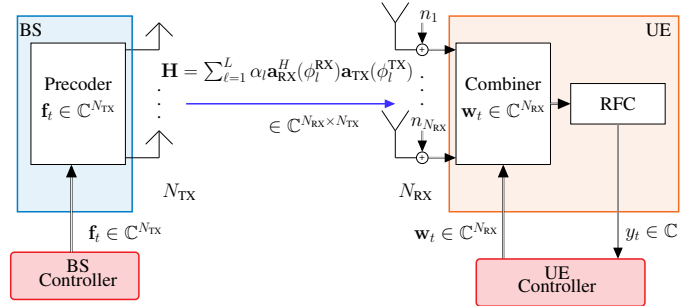


Fig. 1: System model of the proposed BA algorithm. Note how at each timestep t , the beampatterns of BS and UE (i.e., \mathbf{f}_t and \mathbf{w}_t) are determined by a respective control unit (CU), i.e., joint BA is performed.

network (DNN) based beam alignment scheme where first, both basestation (BS) and user equipment (UE) sense the channel using a trainable set of (site-specific) beam-pairs, then the UE feeds back the measurement results to the BS, after which both sides determine their final, grid-free beam-pairs using DNN and the measurement results obtained from the UE. Another approach [10] extends the one-sided adaptive BA scheme of [2] to the joint, two sided BA problem by introducing an adaptive, ping-pong pilot based approach where the role of transmitter (TX) and receiver (RX) are switched after each sensing step, and demonstrates its superior performance over previous state-of-the-art methods in this domain. The work in this paper can be regarded as a combination of [5] (or, by extension, [10]) and [9], which aims to keep current cellular standard compatibility and benefits (like allowing multiple UE to perform BA simultaneously or cell discovery) of [9] while making use of the advantages provided by adaptive BA in [5]. The main contributions of this work are as follows:

- We propose a new end-to-end unsupervised trained, DNN based joint BA algorithm which combines the benefits of a beam-sweep based BA scheme at the BS using learned beam codebooks and adaptive, codebook free BA at the UE side.
- The proposed method can be readily adopted into current cellular standards and can also be used in standalone (SA) architectures.
- We demonstrate the performance of our scheme in various simulations.

This paper is organized as follows: Section II describes

the system model and introduces some important notations. Following this, Section III explains the proposed BA method in more detail. Section IV investigates the performance of the proposed scheme through various experiments. Finally, Section V concludes the paper.

II. PRELIMINARIES

In this paper, we consider the problem of joint, two-sided beam alignment in mmWave communications, i.e., the initial (downlink) communication between a BS and an UE, both equipped with a uniform linear array (ULA) consisting of N_{RX} and N_{TX} antenna elements respectively. Note that in this setup, no initial knowledge about the channel between BS and UE is assumed. In the rest of this paper, we assume that both the UE and the BS are equipped with only a single radio frequency (RF) chain, i.e., analog beamforming and that the transmission channel between UE and BS is static, i.e. constant during each run of the BA algorithm. Furthermore, it is assumed that both the BS and the UE are controlled by CUs which at each discrete timestep t , dictate the current precoding vector $\mathbf{f}_t \in \mathbb{C}^{N_{\text{TX}}}$, and the combining vector $\mathbf{w}_t \in \mathbb{C}^{N_{\text{RX}}}$ at the BS and UE respectively. Also, the CU at the UE also receives the complex valued received symbol $y_t \in \mathbb{C}$ and the current BS beam index $x_t \in \mathbb{Z}$ at each timestep as input. The system model is also depicted in Fig. 1.

A. System Model

As the mmWave channel can be regarded as being spatially sparse, we assume the widely used geometric channel model [11] for the mmWave channel description. Using this model, the channel can be described by:

$$\mathbf{H} = \sum_{\ell=1}^L \alpha_{\ell} \mathbf{a}_{\text{RX}}^H(\phi_{\ell}^{\text{RX}}) \mathbf{a}_{\text{TX}}(\phi_{\ell}^{\text{TX}}) \in \mathbb{C}^{N_{\text{RX}} \times N_{\text{TX}}} \quad (1)$$

for a channel with L paths, complex path gain $\alpha_{\ell} \sim \mathcal{CN}(0, 1)$, angle-of-arrival (AoA) $\phi_{\ell}^{\text{RX}} \sim \mathcal{U}[-\frac{\pi}{2}, \frac{\pi}{2}]$ and angle-of-departure (AoD) $\phi_{\ell}^{\text{TX}} \sim \mathcal{U}[-\frac{\pi}{2}, \frac{\pi}{2}]$ of path ℓ . $\mathbf{a}(\phi)$ describes the array response of the ULA for angle ϕ and is given by

$$\mathbf{a}(\phi) = (1, e^{j\pi \cos(\phi)}, \dots, e^{j\pi(N-1) \cos(\phi)}) \in \mathbb{C}^N \quad (2)$$

with N antennas, and under the assumption of an element spacing of $\frac{\lambda}{2}$. Note that an ULA was chosen as the antenna array geometry due to its simplicity, but other forms like uniform planar arrays (UPAs) are readily integratable as the proposed method is agnostic on the array geometry. Also, as it is assumed that the BS uses only one RF chain and sends a constant stream of pilot symbols with normalized power $P_{\text{TX}} = 1$, the received signal at the UE at timestep t can be described using

$$y_t = \mathbf{w}_t^H \mathbf{H} \mathbf{f}_t + \mathbf{w}_t^H \mathbf{n}_t \in \mathbb{C} \quad (3)$$

with y_t being the complex received symbol at the UE, \mathbf{w}_t being the N_{RX} dimensional complex analog combining vector, \mathbf{f}_t being the N_{TX} dimensional complex analog precoding vector, and noise vector $\mathbf{n}_t \sim \mathcal{CN}(0, \sigma_n^2 \mathbf{I}_{N_{\text{RX}}})$, all for timestep

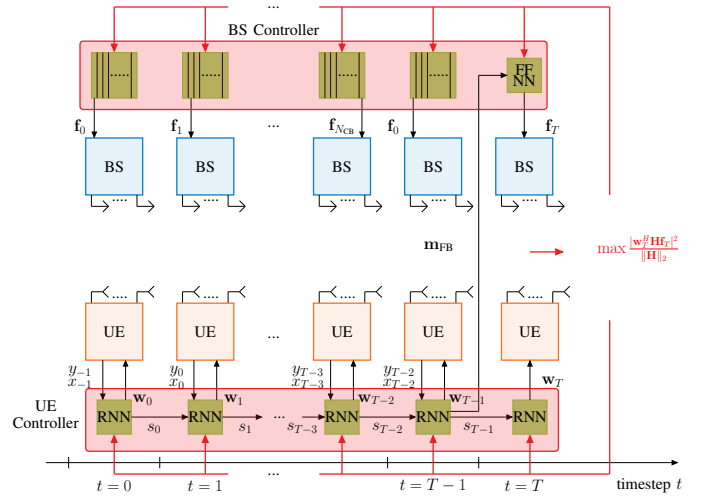


Fig. 2: Unrolled depiction of the proposed joint BA algorithm. For $0 \leq t \leq T-1$ the BS selects its beam based on its learnable codebook, but for $t = T$, the beam is determined codebook free, based on the received feedback \mathbf{m}_{FB} from the UE. Note that green shaded boxes represent trainable components. The red arrow indicates the flow of the gradient used for updating the trainable parameters in the scheme.

t . The receive signal-to-noise-ratio (SNR) after combining for a given \mathbf{w}_t and \mathbf{f}_t is determined as

$$\text{SNR}_{\text{RX}} = \frac{|\mathbf{w}_t^H \mathbf{H} \mathbf{f}_t|^2}{|\mathbf{w}_t^H \mathbf{n}|^2} \quad (4)$$

and the per-antenna $\text{SNR}_{\text{ANT}} = \text{SNR}$ is defined as $\text{SNR} = \frac{1}{\sigma_n^2}$. The (link) satisfaction probability is defined as

$$P_{\text{sat}} = \mathbb{E}_{\mathbf{H}}[\mathbb{1}_{\mathcal{H}_{\text{sat}}}(\mathbf{H})] \quad (5)$$

where $\mathbb{1}$ denotes the indicator function and

$$\mathcal{H}_{\text{sat}} = \{\mathbf{H} : \text{SNR}_{\text{RX}} > \text{SNR}_{\text{threshold}}\} \quad (6)$$

is the set of all channel matrices \mathbf{H} for which the receive SNR at the last timestep is above a threshold value $\text{SNR}_{\text{threshold}}$. In verbal terms, P_{sat} measures the ratio of channels for which the receive SNR of the considered BA scheme satisfies a certain SNR (throughput) threshold. If not mentioned otherwise, in the following, “beamforming gain” refers to the expression $|\mathbf{w}_t^H \mathbf{H} \mathbf{f}_t|^2$. As the channel matrix \mathbf{H} between the UE and BS is not assumed to be known initially, the goal of the proposed scheme is to first collect as much implicit channel state information (CSI) about \mathbf{H} at the UE, and then, use this implicit CSI both at the UE and BS to construct the optimal grid-free final beampair.

III. THE PROPOSED NN BASED SOLUTION

The objective of our proposed scheme is to use the advantages of a codebook-free adaptive BA while keeping the practical benefits that a BS using repeating beam-sweeps offers. The protocol can be divided into three different stages:

- 1) **Channel sensing stage:** The UE initiates the BA process and performs T adaptive sensing steps. During this phase, the BS exhaustively and repeatedly sweeps

through its own codebook with N_{CB} entries (note that in general, T can be larger than N_{CB}). Like in current cellular standards, each BS-beam can be transmitted using reference signals (RSs), like synchronization signal block (SSB) blocks. Furthermore it is also assumed that the UE is always able to extract the beam index out of every SSB beam, irrespective of the SNR after combining.

2) **Feedback determination and final UE beamforming:**

After the T sensing steps, the UE determines

- a) its own predicted best combining vector \mathbf{w}_T
- b) the feedback message $\mathbf{m}_{\text{FB}} \in \mathbb{R}^{N_{\text{FB}}}$ for the BS

The UE then feeds back \mathbf{m}_{FB} to the BS. This can be either done over a lower frequency sidechannel in non-standalone (NSA) systems, or, using \mathbf{w}_T for SA systems (i.e., here the UE transmits and the BS receives).

3) **Final BS beamforming:** The BS uses \mathbf{m}_{FB} to determine its own predicted best combining vector \mathbf{f}_T to use for subsequent communications with the UE.

The unrolled depiction of the proposed algorithm can also be seen in Fig. 2. To utilize the various benefits that neural network (NN) can offer, we use three different kinds of learnable networks: The UE sided recurrent neural network (RNN) (N1), the final beam-mapping network at the BS (N2), and the learnable beam-codebook at the BS (N3). The purpose of these NN is as follows:

- **N1 (RNN):** Sensing network with the goal of obtaining as much CSI information as possible about the channel between BS and UE, based on the measurement sequence of \mathbf{w}_t , y_t and x_t . The obtained information is stored in the internal state s_t . At each timestep t , it outputs a combining vector \mathbf{w}_t , and for $t = T - 1$, it additionally determines a feedback message \mathbf{m}_{FB} for the BS. Also, at the last timestep of the BA process, it outputs the estimated best combining vector \mathbf{w}_T for the UE.
- **N2 (feedforward neural network (FNN)):** Network to map the feedback message \mathbf{m}_{FB} of N1 to the final beampattern \mathbf{f}_T at the BS.
- **N3 (parameter matrix):** Learnable beam-codebook at the BS for possible enhancements over conventionally used codebooks and hardware impairments. This codebook is implemented as a $2 \cdot N_{\text{TX}} \times N_{\text{CB}}$ dimensional trainable parameter matrix as discussed in [9].

N1 is contained inside the UE CU, whereas N2 and N3 are both located inside the BS CU. Formally, the objective of the proposed method is to maximize the following objective function via stochastic gradient-ascent:

$$\max_{\theta_1, \theta_2, \theta_3, \theta_4} \frac{|\mathbf{w}_T^H \mathbf{H} \mathbf{f}_T|^2}{\|\mathbf{H}\|_2} \quad (7)$$

i.e., to maximize the beamforming gain at the final timestep. The objective is normalized by the channel norm (using the Frobenius norm, denoted as $\|\cdot\|_2$) to avoid overemphasis on UEs with good channels [9]. The maximization is subject to the following constraints:

- Unit-norm beamforming vectors:

$$\begin{aligned} \|\mathbf{w}_t\|_2 &= 1 \forall t \\ \|\mathbf{f}_t\|_2 &= 1 \forall t \end{aligned} \quad (8)$$

- Adaptive UE sensing vectors:

$$\mathbf{w}_t = f_{\theta_1}^{\text{UE}}(y_{<t}, x_{<t}, \mathbf{w}_{<t}) \forall t \quad (9)$$

- Codebook based BS precoding vectors in the first T timesteps:

$$\mathbf{f}_t = \mathbf{F}_{\theta_4, [t+i] \bmod N_{\text{CB}},:}^{\text{BS}} \forall 0 \leq t < T \quad (10)$$

- Codebook-free BS precoding vector in the last timestep:

$$\mathbf{f}_T = f_{\theta_3}^{\text{BS}}(\mathbf{m}_{\text{FB}}) \quad (11)$$

- Real valued feedback message \mathbf{m}_{FB} :

$$\mathbf{m}_{\text{FB}} = f_{\theta_2}^{\text{UE}}(y_{<T-1}, x_{<T-1}, \mathbf{w}_{<T-1}) \quad (12)$$

where the superscript BS and UE denotes that the component is used in the transmitter (BS) and receiver (UE), respectively, $y_{-1} = 0$, $x_{-1} = -1$, $\mathbf{w}_{-1} = \mathbf{0}$. $i \in [0, N_{\text{CB}}]$ denotes a random starting index in the BS sided beam codebook to potentially enable the UE to learn a BA algorithm without having to assume a fixed codebook index at the BS, which could reduce the delay of the IA phase in application scenarios. The nonlinear, parameterized functions $f_{\theta_1}^{\text{UE}} : \mathbb{C}^t \times \mathbb{R}^t \times \mathbb{C}^{N_{\text{RX}}t} \rightarrow \mathbb{C}^{N_{\text{RX}}}$, $f_{\theta_2}^{\text{UE}} : \mathbb{C}^{T-1} \times \mathbb{R}^{T-1} \times \mathbb{C}^{N_{\text{RX}}(T-1)} \rightarrow \mathbb{R}^{N_{\text{FB}}}$ are implemented using N1, $f_{\theta_3}^{\text{BS}} : \mathbb{R}^{N_{\text{FB}}} \rightarrow \mathbb{C}^{N_{\text{TX}}}$ by N2 and $\mathbf{F}_{\theta_4, [t+i] \bmod N_{\text{CB}},:}^{\text{BS}} \in \mathbb{C}^{N_{\text{CB}} \times N_{\text{TX}}}$ is the parameterized codebook N3. $\theta_1, \theta_2, \theta_3, \theta_4$ are the vectorized representations of all the learnable parameters in the respective NN. Furthermore, we introduce three different configurations of our proposed BA scheme, using an increasing amount of trainable components:

- **C1:** Here only N1 is assumed to be used, i.e., only the UE side is modified and the BS uses a codebook determined via a conventional optimization method [12]. Consequently, in this case the feedback from UE to BS, namely \mathbf{m}_{FB} , is a single number representing the estimated best BS side beam index and Eq. 12 is slightly modified to:

$$m_{\text{FB}} = \max_k [\sigma(f_{\theta_2}^{\text{UE}}(y_{<T-1}, x_{<T-1}, \mathbf{w}_{<T-1}))_k] \quad (13)$$

where $\sigma : \mathbb{R}^{N_{\text{CB}}} \rightarrow (0, 1)^{N_{\text{CB}}}$ is the N_{CB} dimensional softmax function mapping the N_{CB} dimensional feedback output of N1 to a probability vector. In order to train the learnable parameters of $f_{\theta_2}^{\text{UE}}$, a cross-entropy loss is applied with the one-hot encoding of the optimal BS beam index as label (ground truth) at timestep $t = T - 1$.

- **C2:** This variant is equivalent to variant C1 with the addition of using the learnable map N2.
- **C3:** Here, everything is the same as C2 with the addition of using the learned beam codebook N3, i.e., here all components are learnable.

Configuration	BS beam codebook	BS final beam	UE beampatterns
C1	conventional	conventional	learned
C2	conventional	learned	learned
C3	learned	learned	learned

TABLE I: Summary of the configurations for the proposed scheme.

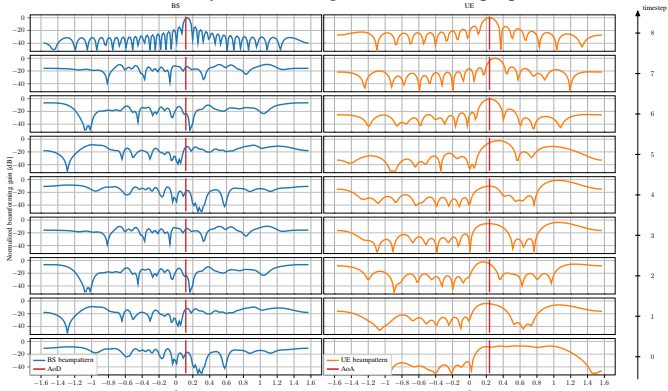


Fig. 3: Unrolled visualization of the learned beampatterns for the proposed joint BA algorithm for a specific channel realization.

Note that variant C1 introduces only a UE-sided modification to the BA process and the BS performs the standard conventional codebook based beam sweeps without any modifications, as also done in current cellular standards. The three introduced configurations are also summarized in Table I. As previously mentioned, the proposed method can be trained straightforward in an end-to-end fashion in the following way: First, sample a random channel matrix according to Eq. 1. Then, unroll the BA algorithm over time using this channel matrix and using equations 3, 8 - 12. Finally, update the trainable weights involved in the computation, $\theta_1, \theta_2, \theta_3, \theta_4$, using back-propagation through time (BPTT) and gradient ascent to maximize the objective of Eq. 7. To stabilize training, the update is averaged over a batch of N_{batch} entries. Due to the modularity of some trainable components (e.g. the learnable codebook $N3$) of the proposed scheme, one can in theory also imagine to train some components independently from each other, e.g. through deep reinforcement learning (DRL).

IV. NUMERICAL RESULTS

Our proposed method will be compared to the following baselines:

- **Exhaustive Search:** Both the BS and UE exhaustively sweep through a equal beam-width-codebook generated by a conventional optimization algorithm [12] after which the beam-pair obtaining the highest power is chosen. M_{TX} (M_{RX}) denotes the number of beampatterns in the BS (UE)-sided codebook. For fairness of comparison, $M_{\text{TX}} \cdot M_{\text{RX}} = T$.
- **Maximum ratio transmission (MRT) and maximum ratio combining (MRC):** This is the theoretical upper bound for the given scenario where the BS uses the MRT precoding vector and the UE the MRC combining vector.
- **Joint, non-adaptive (DNN_{NOA}):** A DNN-based scheme as introduced in [9], where both the BS and UE jointly sweep through a set of learned beampairs, after which

the UE feeds back the measurement results and both sides determine a grid-free final beampair based on these measurement results.

- **Joint, adaptive (RNN_A):** A RNN-based ping-pong scheme as introduced in [10], where both the BS and UE jointly perform adaptive, codebook-free BA, and switch the role of TX and RX after each timestep. Note that here one timestep t refers to one “channel use”, i.e., in each timestep one side transmits and the other side receives.

Note that DNN_{NOA} can be seen as an approach where both parties of the BA procedure are codebook-bound (except for the last beam-pair), non-adaptive and in RNN_A, both sides perform codebook-free, adaptive BA, whereas our approach has one side (i.e., the BS) non-adaptive, codebook-based and the other side (i.e., the UE) codebook-free, non-adaptive. As the focus here lies on comparing the performance of the high-level schemes, the loss functions of both DNN_{NOA} and RNN_A were set to the same loss-function also used for the proposed method (without any auxiliary losses), i.e. the implementations used in this paper slightly differ from those of the original proposals. Also note that for ease of explanation and simplicity, both the UE of the proposed method and RNN_A do not use a separate DNN to determine the final beam(s) at the last timestep. An overview over the high level characteristics of the baselines is also shown in Table II. In the following experiments, if not mentioned otherwise, $L = 3$, $N_{\text{TX}} = 32$, $N_{\text{RX}} = 16$, $N_{\text{CB}} = 8$, batch size $N_{\text{batch}} = 1024$, and the training SNR is set to 10 dB. Also, the threshold value $\text{SNR}_{\text{threshold}}$ is set to 20 dB and the dimension of \mathbf{m}_{BF} , N_{FB} , is set to 16. Furthermore, the amount of trainable parameters in the tested NN based schemes is set to be roughly 500K. The RNNs used for the UE side (N1) in this scheme consists of two layers of gated recurrent units (GRUs) [13] whereas components (e.g. N2) employing feedforward networks consist of two to three layers of fully connected DNN.

Fig 3 aims to provide a visualization of the learned BA algorithm for $L = 1$, $T = 8$ and $N_{\text{CB}} = 4$ (i.e., 8 UE-sensing steps), and for configuration C3. Plotted are the normalized beamforming gains of the beampatterns (calculated using $|\mathbf{v}^H \mathbf{a}(\phi)|^2$ with $\phi \in [-\frac{\pi}{2}, \frac{\pi}{2}]$ and combining (precoding) vector \mathbf{v}) used by the BS (marked in blue) and UE (marked in orange) during the BA process. It can be clearly seen that in the first stages of the BA process, the UE senses the channel with relatively wide beampatterns, whereas for the later timesteps of the algorithm, the search area of the UE is narrowed down and more energy is focused in certain directions. Also note the repeating BS-sided beampatterns in the first 8 timesteps, caused by its codebook-based beamsweep.

In a first experiment, we want to investigate the effects of the various learnable components on the performance of the proposed BA procedure, i.e., we want to investigate the performance of C1, C2 and C3, as described in the previous section. The results are shown in Fig. 4, $T = 16$. One can observe that all three tested variants outperform the exhaustive search by at least 10 dB and that introducing an increasing amount of learnable components into the scheme improves the

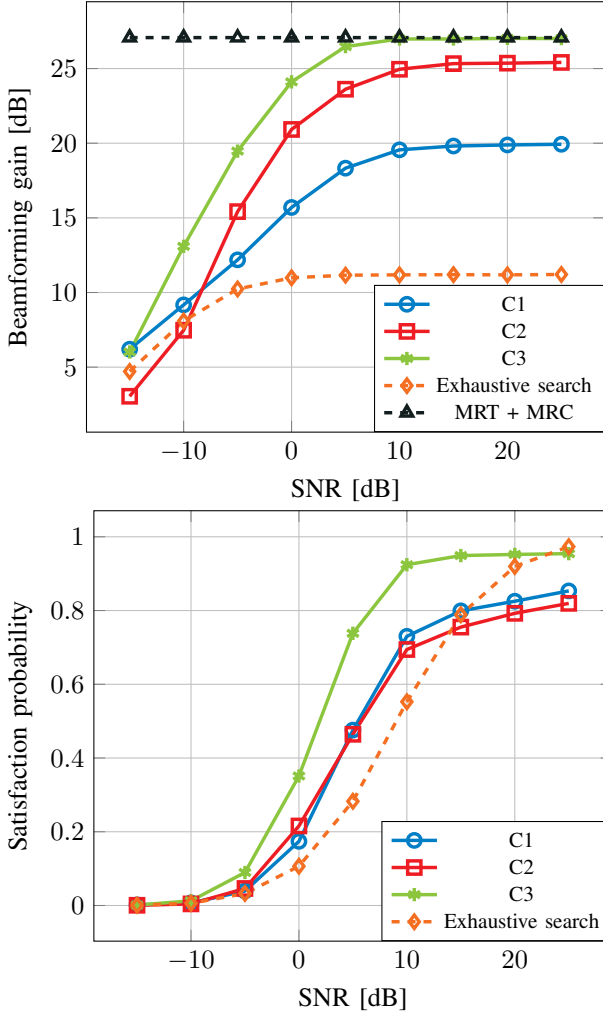


Fig. 4: Comparison of the performance impact of the various NNs used in the proposed scheme, top: beamforming gain versus SNR, bottom: satisfaction probability versus SNR.

performance. Also remarkable is the large benefit in regards to satisfaction probability when introducing a learnable beam-codebook at the BS.

Another aspect we want to examine is the impact of T , i.e., the number of sensing steps, on the performance for a fixed N_{CB} , i.e., the potential benefit of additional beam alignment steps after the UE has observed all N_{CB} beams of the BS. To also investigate the influence of the learnable codebook on the performance (especially if $T \leq N_{CB}$), the experiment is performed for both the variants C2 and C3. For this experiment, the parameters of the system are chosen to be identical to those of the previous experiment, and the per-antenna SNR, SNR_{ANT} , is held constant to 5 dB. The results are displayed in Fig. 5. One can observe that while the performance of both tested variants increases steadily by increasing T , the gap in their performance between allowing one and more sensing steps also increases. Also visible is the general large increase both in the achievable beamforming gain and satisfaction probability if a learned beam-codebook is introduced into the scheme, especially for small $T < N_{CB}$.

In two further experiments, the performance of the proposed

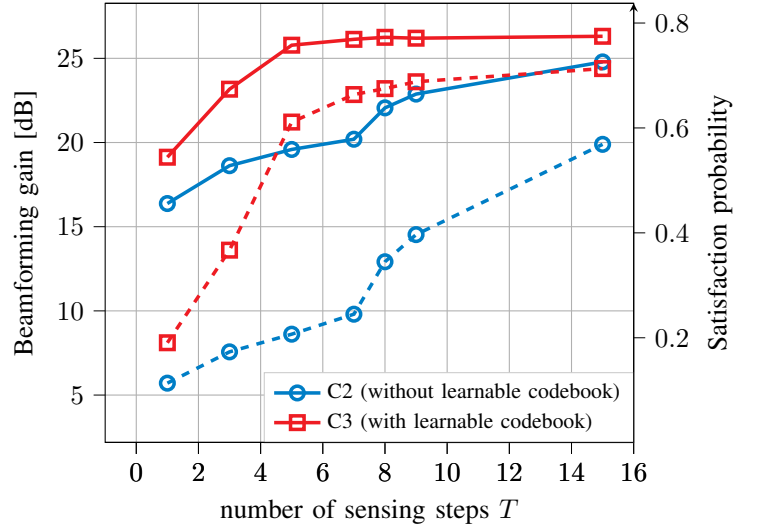


Fig. 5: Comparison of the performance impact of varying T for fixed $N_{CB} = 8$ for the proposed scheme. Solid lines: beamforming gain versus T , dashed lines: satisfaction probability versus T .

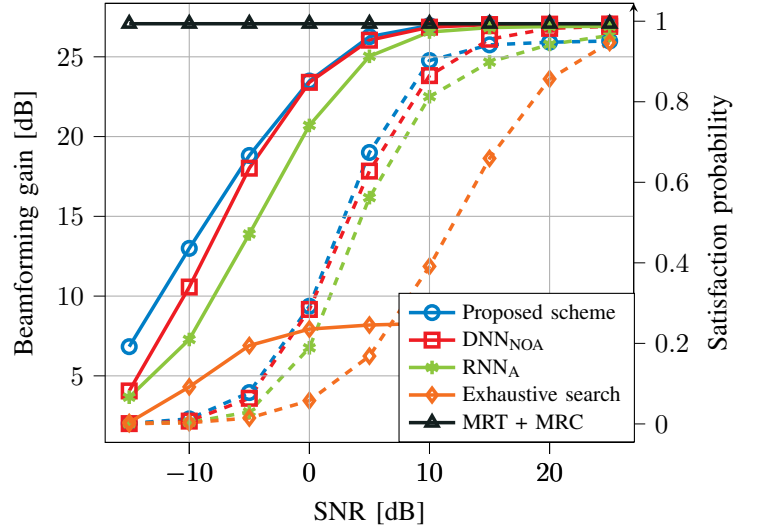


Fig. 6: Performance of different BA schemes for fixed $T = 8$ and different values of testing SNR_{ANT} . Shown are the beamforming gain (solid) and the satisfaction probability (dashed).

scheme in comparison to several relevant baselines is investigated. To keep the comparison fair, in this experiment, the starting beam-codebook index i of the proposed scheme is fixed to 0. In the first experiment, the amount of sensing steps, T , is fixed to 8 for all schemes. The results are shown in Fig. 6. As can be seen, all tested DNN-based schemes outperform the exhaustive search baseline in average beamforming gain by orders of magnitude. Our proposed scheme slightly beats all tested baselines both in achieved beamforming gain and satisfaction probability in this experiment, even RNN_A. The performance improvements of our proposed scheme in comparison to DNN_{NOA} might be attributed to the adaptiveness at the UE side whereas the difference to RNN_A might be caused by the differing feedback schemes. These observations also hold in a next experiment: Here we now fix the training and testing SNR to $\text{SNR}_{\text{ANT}} = 5$ dB, and vary the amount

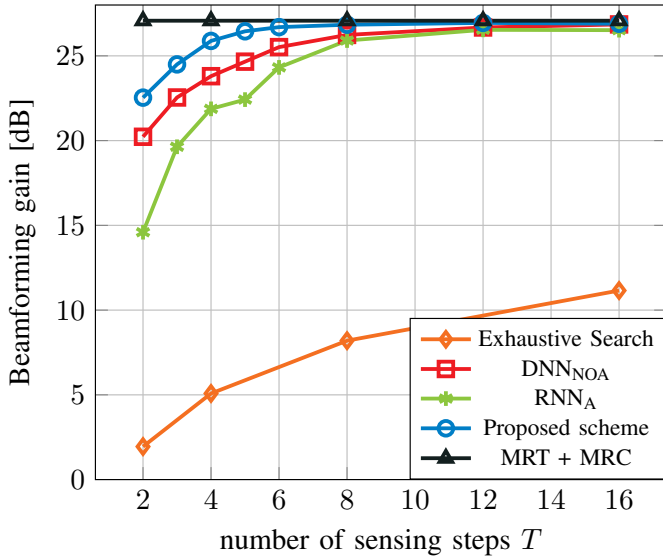


Fig. 7: Beamforming gain versus number of sensing steps T of different BA schemes for fixed $\text{SNR}_{\text{ANT}} = 5$ dB.

BA scheme	BS method	BA method	UE method	BA method	Beam sweeping overhead	Feedback overhead
Exhaustive search	NOA, SEQ	NOA, SEQ	NOA, SEQ		$M_{\text{TX}}M_{\text{RX}}$	K beam indices
DNN _{NOA}	NOA, JOINT	NOA, JOINT	NOA, JOINT		T	$K \cdot T$ power values
RNN _A	A, JOINT	A, JOINT	A, JOINT		$K \cdot T$	0
Proposed	NOA, JOINT	A, JOINT	A, JOINT		T	$K N_{\text{FB}}$ real valued numbers

TABLE II: Overview over the compared approaches together with their beam sweeping and feedback overhead for K UE. “NOA” = non-adaptive, “A” = adaptive, “SEQ” = sequential, “JOINT” = joint.

of sensing steps T . For the learnable schemes, a different NN is trained for each T , and for the proposed scheme, the codebook-size at the BS, N_{CB} , is set to 8. Fig. 7 shows the results. Here again, the differences in the achieved average beamforming gain between the tested schemes become visible, most likely due to the previously mentioned reasons. Also noteworthy is that all tested learned schemes at $T = 2$ already outperform the exhaustive search baseline at $T = 16$ sensing steps in regard to achieved average beamforming gain. Note however that the exhaustive search-based scheme has the lowest computational complexity out of the tested schemes and further investigations into the performance-complexity trade-off of the NN based schemes might be beneficial. Furthermore, due to the codebook-sweep based BS in our proposed scheme, in theory many UE can perform BA in parallel. The overhead of the various methods for alignment of K UE in terms of required pilots and feedback signals is also shown in Tab. II. Note that experiments showed that a small number of N_{FB} seems to be sufficient to enable good performance and thus, N_{FB} could be expected to stay well below T .

V. CONCLUSION

We propose a novel deep learning based initial access joint beam alignment scheme with combines the advantages offered

by adaptive, codebook free beam alignment at the UE and codebook based beam sweeping at the BS. The introduced scheme is trainable in an end-to-end fashion and is shown to offer superior performance to purely codebook-sweep based methods. It is designed in such a way that it can be readily applied in existing beam sweeping-based frameworks without requiring modifications to the alignment process. Furthermore, our scheme does not rely on starting on a fixed codebook beam from the BS, and thus, can start the beam alignment process anytime without having to wait for a specific BS codebook beam to appear. There are various possible future directions this line of research could be extended: For example, one could try to train the UE using the deep reinforcement learning framework to adaptively terminate the BA process depending on the channel and the target receive SNR without having a fixed T in order to save redundant sensing steps. One could also investigate and study the behaviour and possible extension of the proposed scheme to situations where the BS employs codebooks not encountered during training.

REFERENCES

- [1] A. Alkhateeb, O. El Ayach, G. Leus, and R. W. Heath, “Channel Estimation and Hybrid Precoding for Millimeter Wave Cellular Systems,” *IEEE Journal of Selected Topics in Signal Processing*, vol. 8, no. 5, pp. 831–846, 2014.
- [2] S.-E. Chiu, N. Ronquillo, and T. Javidi, “Active Learning and CSI Acquisition for mmWave Initial Alignment,” *IEEE Journal on Selected Areas in Communications*, vol. 37, no. 11, pp. 2474–2489, 2019.
- [3] H. Hassanieh, O. Abari, M. Rodriguez, M. Abdelghany, D. Katabi, and P. Indyk, “Fast Millimeter Wave Beam Alignment,” in *Proceedings of the 2018 Conference of the ACM Special Interest Group on Data Communication*, ser. SIGCOMM ’18. New York, NY, USA: Association for Computing Machinery, 2018, p. 432–445.
- [4] F. Sohrabi, Z. Chen, and W. Yu, “Deep Active Learning Approach to Adaptive Beamforming for mmWave Initial Alignment,” *IEEE Journal on Selected Areas in Communications*, vol. 39, no. 8, pp. 2347–2360, 2021.
- [5] F. Sohrabi, T. Jiang, W. Cui, and W. Yu, “Active Sensing for Communications by Learning,” *IEEE Journal on Selected Areas in Communications*, vol. 40, no. 6, pp. 1780–1794, 2022.
- [6] D. Tandler, S. Doerner, M. Gauger, and S. ten Brink, “Deep reinforcement learning for mmwave initial beam alignment,” in *WSA & SCC 2023; 26th International ITG Workshop on Smart Antennas and 13th Conference on Systems, Communications, and Coding*, 2023, pp. 1–6.
- [7] I. Chafaa, E. V. Belmaga, and M. Debbah, “One-bit feedback exponential learning for beam alignment in mobile mmwave,” *IEEE Access*, vol. 8, pp. 194 575–194 589, 2020.
- [8] —, “Adversarial Multi-armed Bandit for mmWave Beam Alignment with One-Bit Feedback,” in *VALUETOOLS 2019: 12th EAI International Conference on Performance Evaluation Methodologies and Tools*. Palma Spain, France: ACM, 2019, pp. 23–30. [Online]. Available: <https://hal.science/hal-03160015>
- [9] Y. Heng and J. G. Andrews, “Grid-free mimo beam alignment through site-specific deep learning,” 2022.
- [10] T. Jiang, F. Sohrabi, and W. Yu, “Active sensing for two-sided beam alignment using ping-pong pilots,” in *2022 56th Asilomar Conference on Signals, Systems, and Computers*, 2022, pp. 913–918.
- [11] O. E. Ayach, S. Rajagopal, S. Abu-Surra, Z. Pi, and R. W. Heath, “Spatially sparse precoding in millimeter wave mimo systems,” *IEEE Transactions on Wireless Communications*, vol. 13, no. 3, pp. 1499–1513, 2014.
- [12] J. Song, J. Choi, and D. J. Love, “Codebook design for hybrid beamforming in millimeter wave systems,” in *2015 IEEE International Conference on Communications (ICC)*, 2015, pp. 1298–1303.
- [13] K. Cho, B. van Merriënboer, C. Gulcehre, D. Bahdanau, F. Bougares, H. Schwenk, and Y. Bengio, “Learning phrase representations using rnn encoder-decoder for statistical machine translation,” 2014.